Enhancing the thermoelectric properties of 2D Bi_2Se_3 by 1D texturing with graphene

Jen-Kai Wu, Mario Hofmann, Wen-Pin Hsieh, Szu-Hua Chen, Zhi-Long Yen, Sheng-Kuei Chiu, Yi-Ru Luo, Yuan-Huei Chang, Ya-Ping Hsieh**

Mr. Jen-Kai Wu, Ms. Szu-Hua Chen, Mr. Zhi-Long Yen, Prof. Mario Hofmann, Prof. Yuan-Huei Chang, Department of Physics, National Taiwan University, Taipei 10617, Taiwan

Prof. Mario Hofmann, Prof. Yuan-Huei Chang

Graduate Institute of Applied Physics, National Taiwan University, Taipei 10617, Taiwan

Prof. Wen-Pin Hsieh

Institute of Earth Sciences, Academia Sinica, Taipei 11529, Taiwan

Dr. Sheng-Kuei Chiu, Prof. Ya-Ping Hsieh

Institute of Atomic and Molecular Sciences, Academia Sinica, Taipei 10617, Taiwan

Email: yphsieh@gate.sinica.edu.tw (Y. P. Hsieh)

Mr. Yi-Ru Luo

Institute of Opto-Mechatronics, National Chung Cheng University, Chiayi 62102, Taiwan

Corresponding Author

*Prof. Y. H. Chang Email: yhchang@phys.ntu.edu.tw

*Prof. Y. P. Hsieh Email: yphsieh@gate.sinica.edu.tw

1. Crystallinity

A typical logarithmic XRD pattern of BSG can be seen in the Figure S1. The sharp (003) family peaks indicates a crystalline Nano-flakes, and all (003) family can be indexed for rhombohedral structure of Bi_2Se_3 with $R\bar{3}m$ space group with lattice parameters c = 28.57 Å.[1] There is obviously no impurity peak detected which implies that high quality of Bi_2Se_3 deposited on graphene.

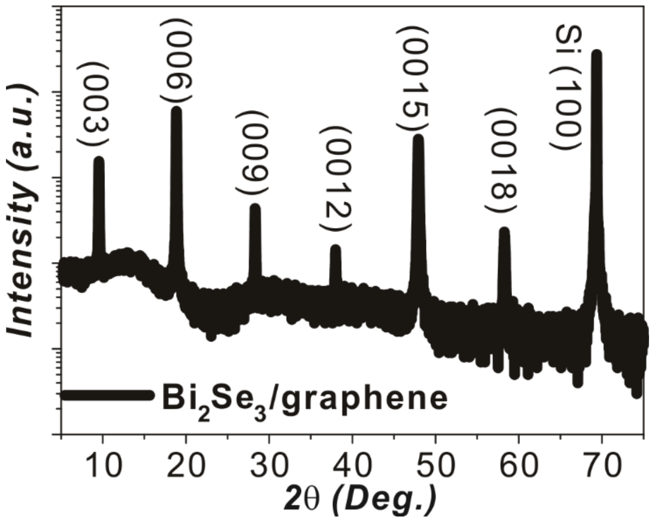

Figure S1. The XRD patterns of BSG.

2. Stoichiometric Composition

To understand the chemical stoichiometry of our BSG, XPS spectra (with Mg Kα/Al Kα x-ray source) were analyzed. Figure S2a shows the selenium 3d spectra which consists of two peaks, 53.5 eV and 54.4 eV that correspond to Se $3d_{5/2}$ and Se $3d_{3/2}$, respectively. The XPS spectra of Bi 4f core level as shown in the Figure S3b, which reveals two spin-orbit doublet components with peak position at about 158.1 eV and 163.4 eV that corresponds to Bi $4f_{7/2}$ and Bi $4f_{5/2}$, respectively. The spin orbit doublet a weak intensity peak additionally overlapped with the spectrum of Bi 4f spectra and fitted by Gaussian function which corresponds to Se $3p_{3/2}$ (159.3 eV) and Se $3p_{1/2}$ (164.8 eV). The phenomenon is consistent with previous reports that regions of Bi 4f and Se 3d have well separated spin-orbit components which are $\Delta = 5.3$ eV and $\Delta = 0.86$ eV.[2] We use CASAXPS software to analyze the chemistry stoichiometry of Bi and Se. The ratio of the atomic percentage of a_{Bi} and a_{Se} can be estimated through the following equation:

$$a_{Bi} : a_{Se} = \frac{A_{\mathrm{Bi4f}}}{s_{\mathrm{Bi4f}}} : \frac{A_{\mathrm{Se3d}}}{s_{\mathrm{Se3d}}},$$

where a is the atomic percentage, A is area of the integrated intensity, and s is the atomic sensitivity factor, which convert the relative peak areas to the relative numbers of atoms in the detected area.[3] By introducing the calculated areas of Bi 4f and Se 3d with s_{Bi4f} (9.14) and s_{Se3d} (0.853) for x-ray sources at 54.7°, we obtain the atomic percentage of Bi and Se is 40.96 % to 59.04 % which is very close to 2 to 3. Thus, XPS spectrum demonstrates our sample possesses pure Bi_2Se_3 Nano-flakes grown on G/SiO_2/Si substrate.

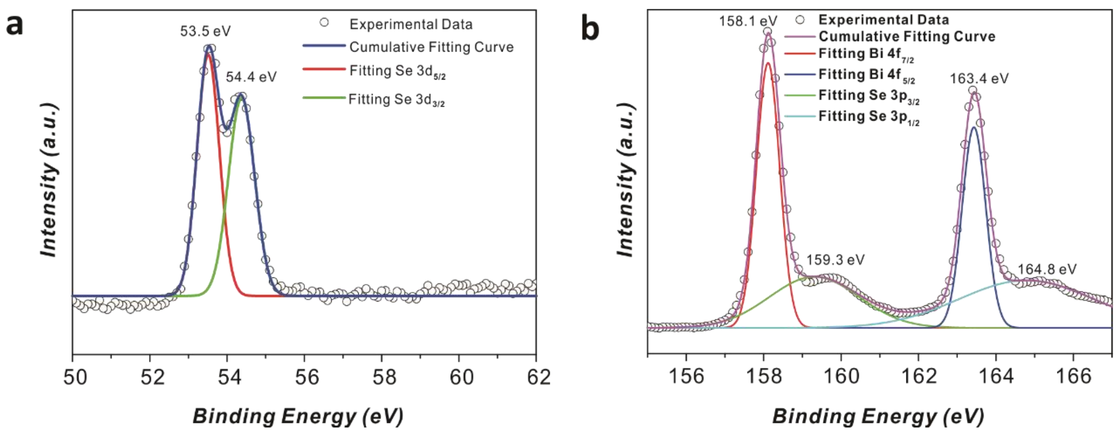

Figure S2. The electron core level of (a) Se 3p and (b) Bi 4f.

3. Extraction of thermal conductance from Seebeck voltage vs. temperature and comparison to experimental results

Following Roh *et al.*,[4] we characterize the Seebeck voltage as a function of sample temperature and obtain a linear relationship that is divided into slope (a) and intercept(b).

$$\Delta V_{SB} = \frac{\alpha^2 T I}{G} - \frac{I^2 \alpha R_M}{2G} = aT + b$$

Using the experimentally obtained values in Figure 2(b) we can extract a ratio of thermal conductance (G) for 3D and 2D Bi_2Se_3 samples.

$$\frac{G_{3D}}{G_{2D}} = \frac{a_{3D} R_{3D}^2}{a_{2D} R_{2D}^2} \frac{b_{2D}^2}{b_{3D}^2}$$

We obtain a thermal conductance ratio of approximately 1.05 which is in relatively good agreement with the extracted thermal conductance ratio (1.5).

4. Extraction of Seebeck coefficient from Seebeck voltage vs. temperature and comparison to experimental results

Using the same approach, we can extract the Seebeck coefficient for 2D Bi_2Se_3

$$\alpha = \frac{aIR}{2b} \sim 20 \ \frac{\mu\text{V}}{\text{K}}$$

This result agrees well with the value measured on macroscopic samples (32.053 μV K^{-1})

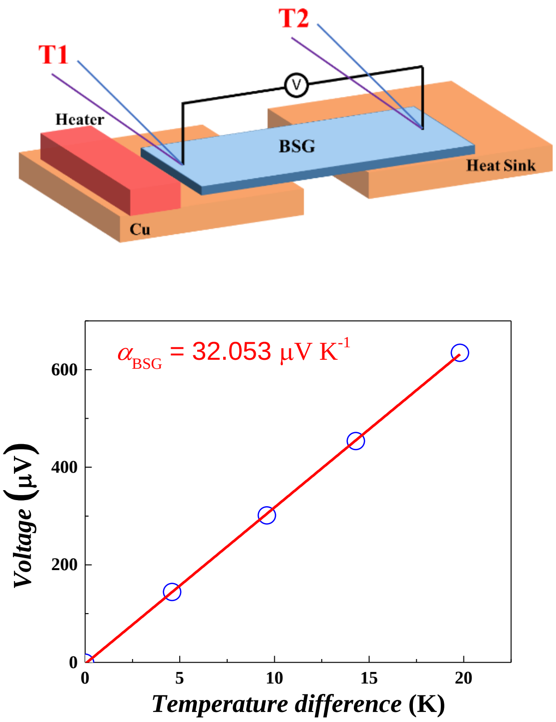

Figure S3. The schematic of traditional (differential method) measurement (top) and Seebeck voltage vs. temperature difference of BSG (bottom).

5. Extended AFM characterization

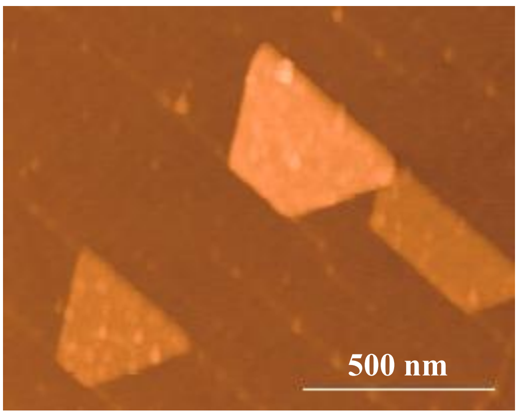

Figure S4. Trapezoidal shapes of Bi_2Se_3 for longer growth time.

6. Schematic of experimental process

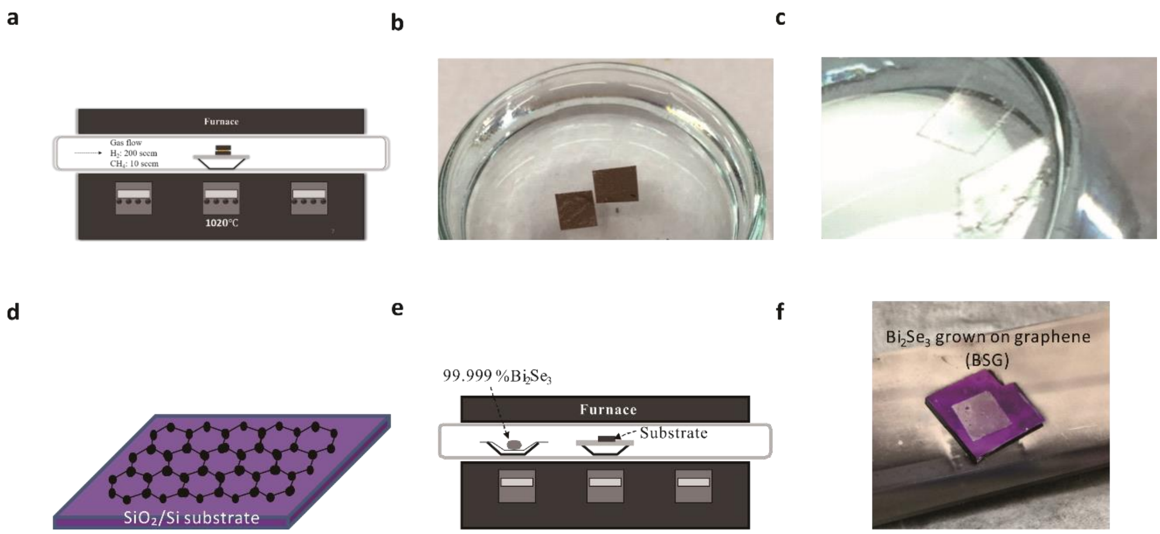

Figure S5. (a-e) The schematic diagram and photograph of our experimental setup. (f) The photograph of BSG.

7. Electrical conductivity and thermal conductivity changes with temperature

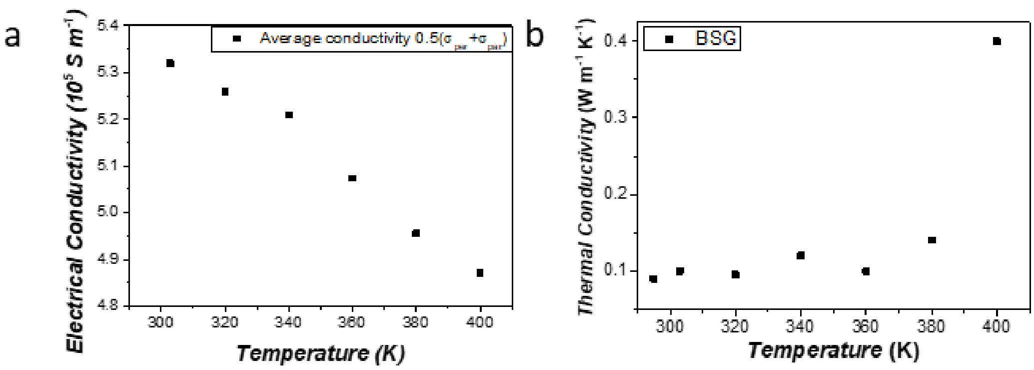

Figure S6. (a) Electrical conductivity and (b) thermal conductivity changes with temperature of BSG.

8. Schematic of measurement directions

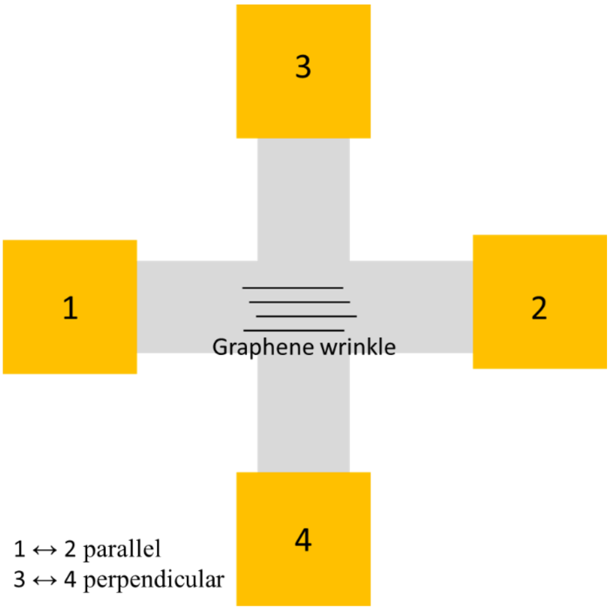

Figure S7. The schematic of measurement direction of cross-structure BSG.

9. TDTR measurement schematics

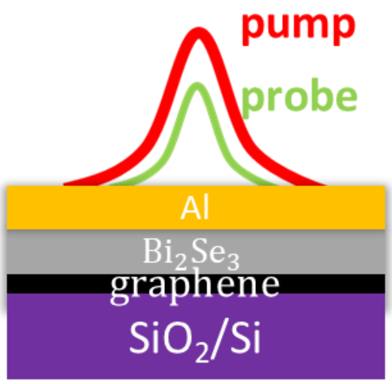

Figure S8. The schematic of a typical thin film measured using TDTR technique.

References

(1) Zhang, C.; Liu, M.; Man, B. Y.; Jiang, S. Z.; Yang, C.; Chen, C. S.; Feng, D. J.; Bi, D.; Liu, F. Y.; Qiu, H. W.; Zhang, J. X., Facile fabrication of graphene-topological insulator Bi_2Se_3 hybrid Dirac materials via chemical vapor deposition in Se-rich conditions. *CrystEngComm* **2014,** *16* (38), 8941-8945.

(2) Sun, Y.; Cheng, H.; Gao, S.; Liu, Q.; Sun, Z.; Xiao, C.; Wu, C.; Wei, S.; Xie, Y., Atomically Thick Bismuth Selenide Freestanding Single Layers Achieving Enhanced Thermoelectric Energy Harvesting. *J. Am. Chem. Soc.* **2012,** *134* (50), 20294-20297.

(3) Lee, H.-Y.; Chen, Y.-S.; Lin, Y.-C.; Wu, J.-K.; Lee, Y.-C.; Wu, B.-K.; Chern, M.-Y.; Liang, C.-T.; Chang, Y. H., Epitaxial growth of Bi_2Te_3 topological insulator thin films by temperature-gradient induced physical vapor deposition (PVD). *J. Alloys Compd.* **2016,** *686*, 989-997.

(4) Roh, I.-J.; Lee, Y. G.; Kang, M.-S.; Lee, J.-U.; Baek, S.-H.; Kim, S. K.; Ju, B.-K.; Hyun, D.-B.; Kim, J.-S.; Kwon, B., Harman Measurements for Thermoelectric Materials and Modules under Non-Adiabatic Conditions. *Sci. Rep.* **2016,** *6* (1), 39131.